Cell Reports, Volume *43*

Supplemental information

Carcinoma-associated mesenchymal stem cells promote ovarian cancer heterogeneity and metastasis through mitochondrial transfer

Leonard Frisbie, Catherine Pressimone, Emma Dyer, Roja Baruwal, Geyon Garcia, Claudette St. Croix, Simon Watkins, Michael Calderone, Grace Gorecki, Zaineb Javed, Huda I. Atiya, Nadine Hempel, Alexander Pearson, and Lan G. Coffman

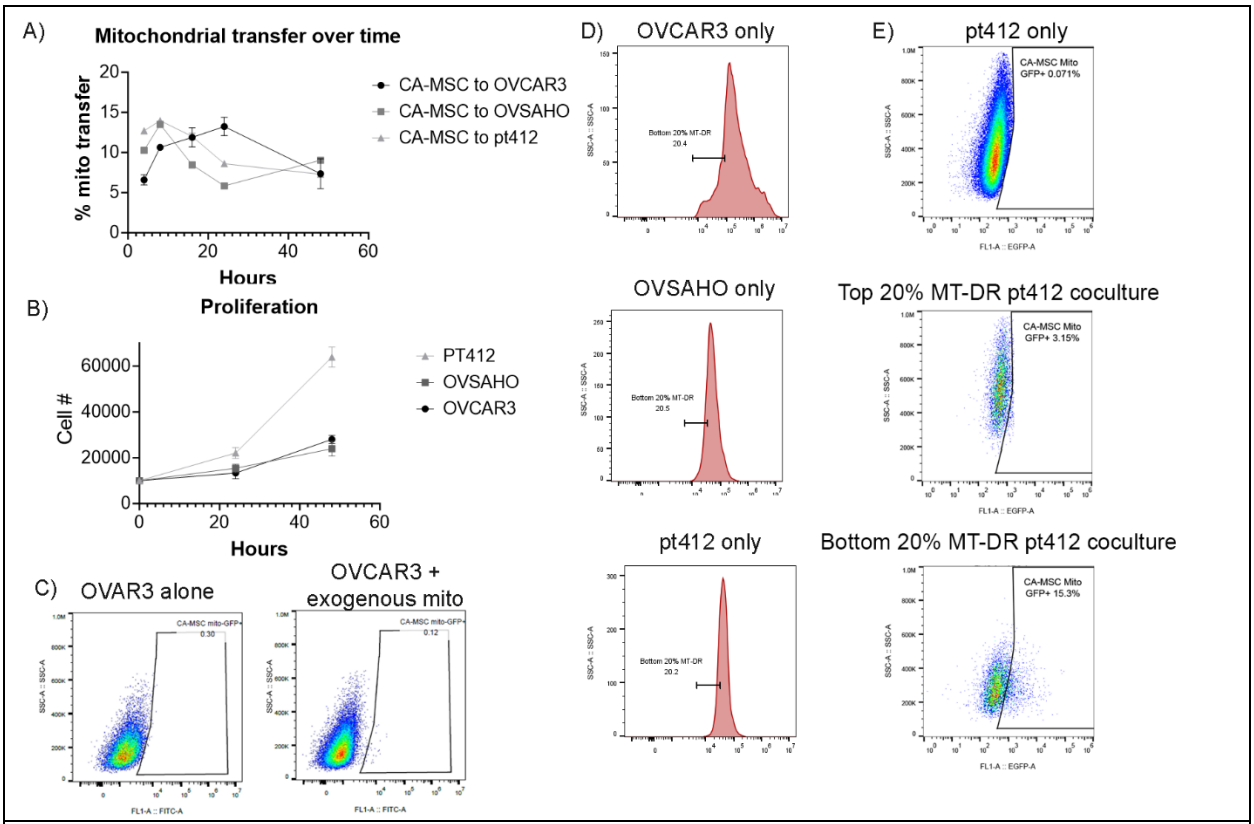

Figure S1. Mitochondrial transfer overtime and gating strategy for identification of CA-MSC mitochondrial transfer, related to Figure 2. A) Percent CA-MSC to tumor cell (OVCAR3 vs OVSAHO vs pt412) over time. B) Baseline proliferation rates of tumor cells grown alone. C) OVCAR3 tumor cells alone or after 5 min spike in of isolated GFP-mitochondria, wash, then flow analysis to control for external mitochondria sticking to cell surface. D) Baseline distribution of active mitochondria (labeled with MitoTracker Deep Red) in OVCAR3, OVSAHO and pt412 cells grown alone. E) Identification of 'mito poor' and 'mito rich' tumor cell subpopulations using MitoTracker Deep Red and stromal cell mitochondrial transfer using coculture with CA-MSC GFP labeled mitochondria.

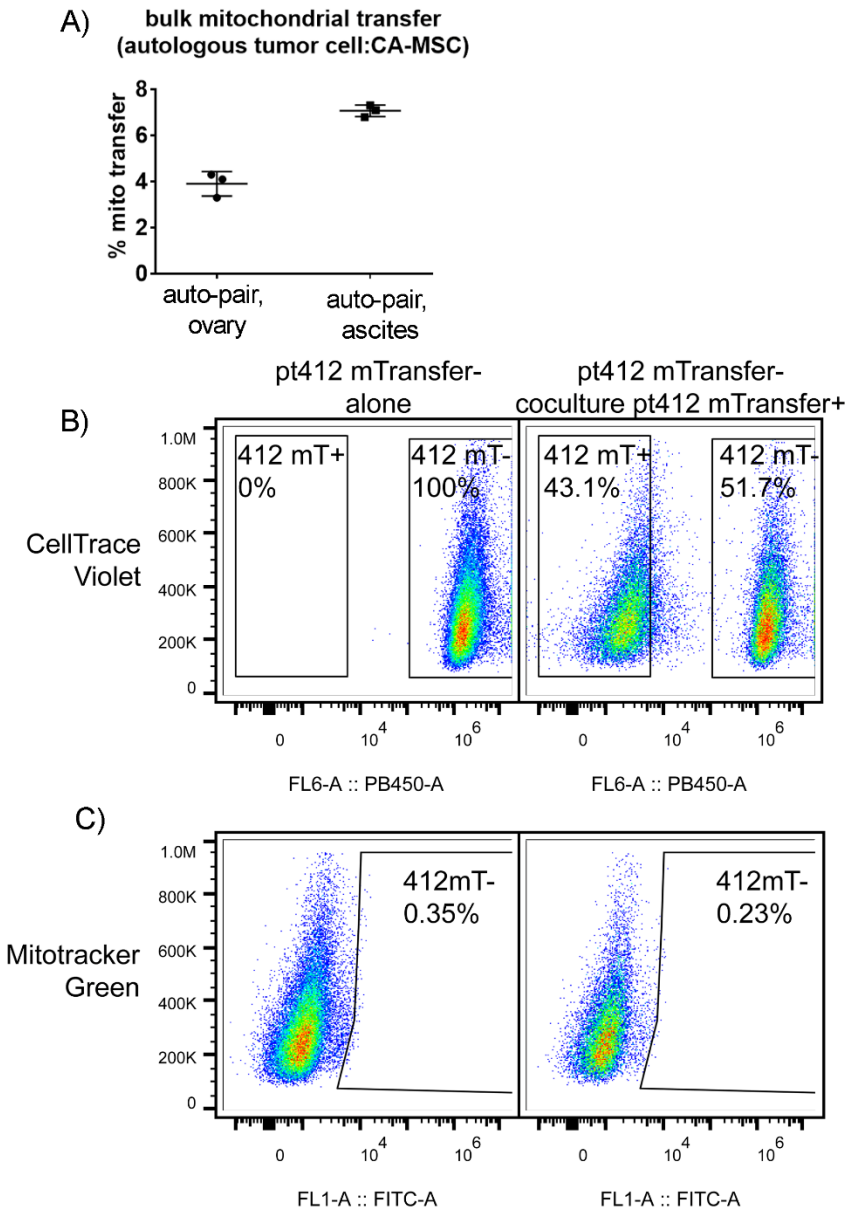

Figure S2. Quantification of mitochondrial transfer from paired, autologous tumor cell and CA-MSC samples. Seahorse analysis of exogenously added mitochondria. 'Mito Poor' pt412 cells receiving CA-MSC mitochondria do not transfer mitochondria to other 'Mito Poor' pt412 cells not receiving CA-MSC mitochondria, related to Figure 4. A) CA-MSCs and tumor cells were isolated from the same patient (first pair derived from an ovary sample, the second pair derived from ascites). CA-MSC mitochondria were labeled with mito-green and mitochondrial transfer from the paired CA-MSC and tumor cell samples were quantified using flow cytometry**.** B) FACS isolated pt412 tumor cells which received mitochondria from CA-MSCs (mT+) labeled with MitoTracker Green were grown with FACS isolated pt412 tumor cells which did not receive mitochondria (mT-). C) After co-culture, the mT- tumor cells did not gain mitochondria from the mT+ tumor cells indicating tumor cells do not transfer either endogenous or donated mitochondria to other tumor cells

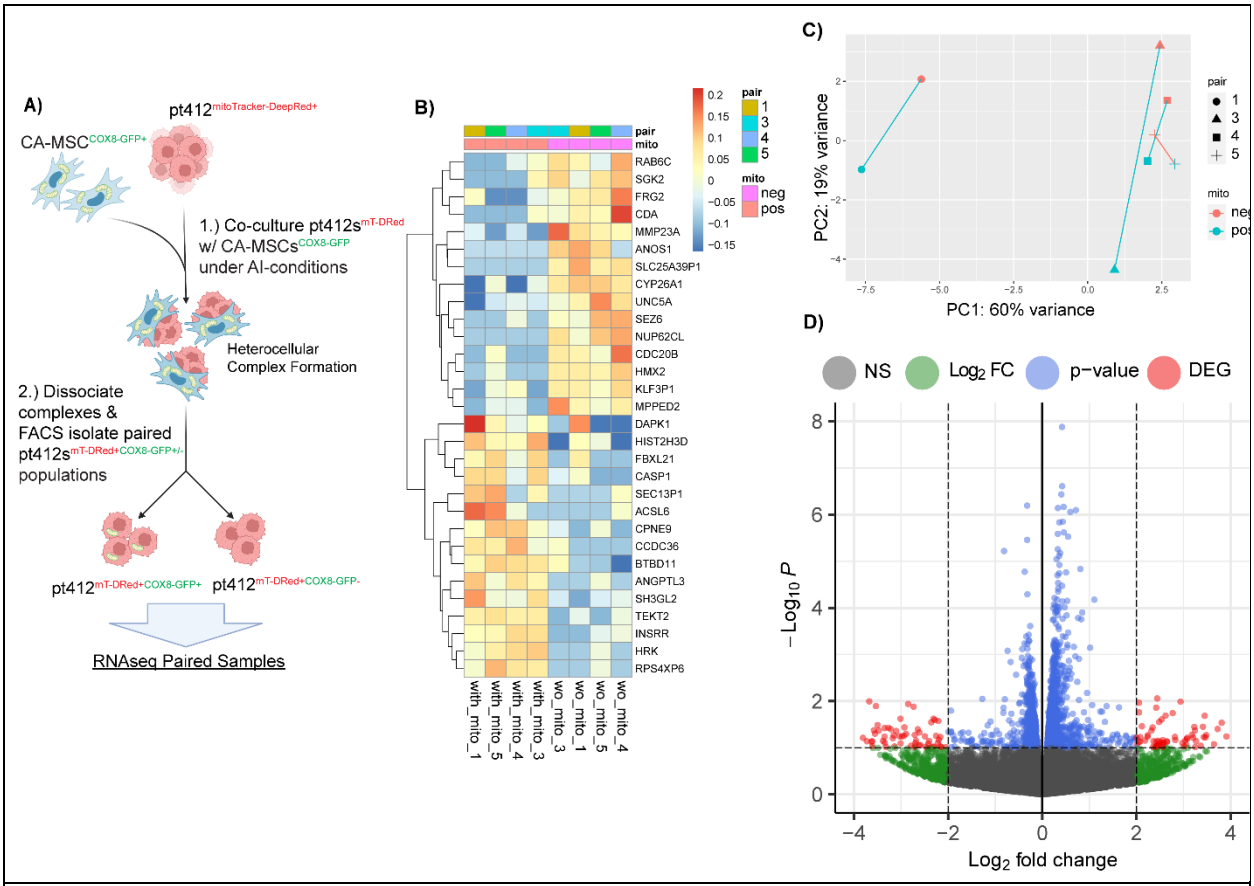

Figure S3. RNA Sequencing and differential expression analysis of +mitoTransfer / -mitoTransfer pt412 tumor cell pairs, related to Figure 4. A) Diagram outlining the isolation of paired +mitoTransfer/-mitoTransfer pt412 cells for RNAseq. B) Heatmap of top differentially expressed mRNAs in +mitoTransfer pt412 cells (*n*=4 paired samples). C) PCA plot of pt412 sample pairs. D) Volcano plot highlighting DEGs identified in +mitoTransfer pt412 cells.

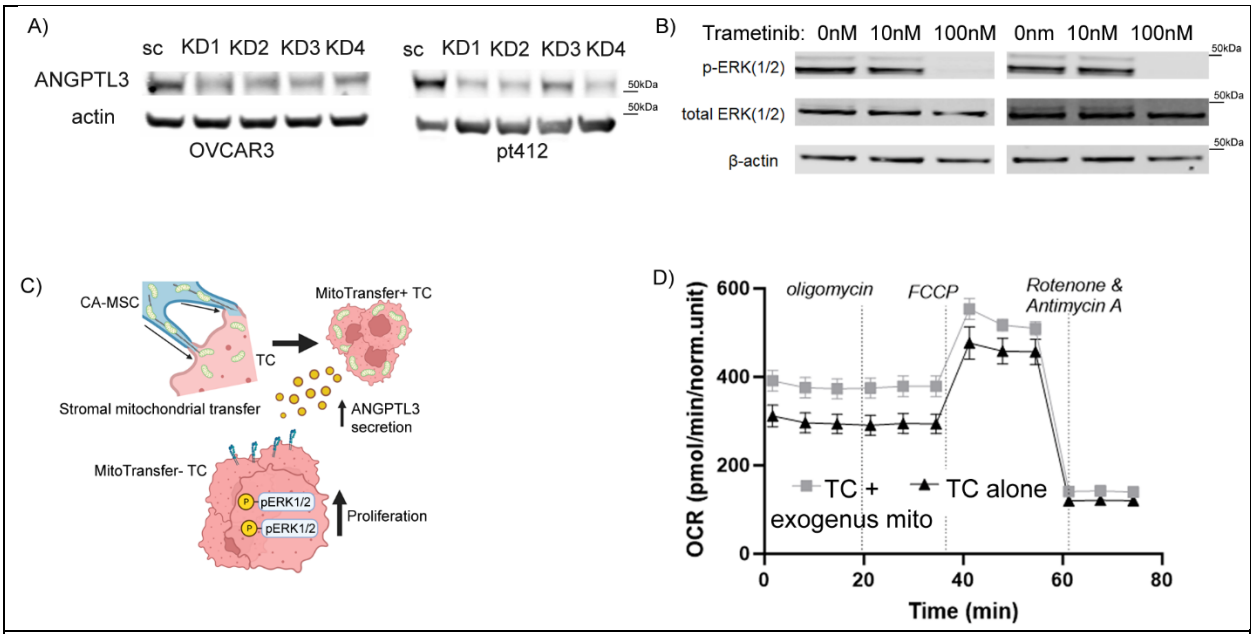

Figure S4. Validation of ANGPTL3 knockdown (KD) and dose dependent decrease in pERK with Trametinib, related to Figure 4. A) Western blot of ANGPTL3 in OVCAR3 and pt412 tumor cells using four independent shRNA ANGPTL3 clones (KD1-KD4) compared to scrambled control (SC). B) Western blot of pERK(1/2) vs total ERK(1/2) and actin in OVCAR3 and pt412 after treatment with increasing doses of Trametinib. C) Cartoon rendering of proposed mechanism of action. D) Live mitochondria isolated from CA-MSC were added to tumor cells and a portion were engulfed by tumor cells resulting in increased oxidative phosphorylation in tumor cells.

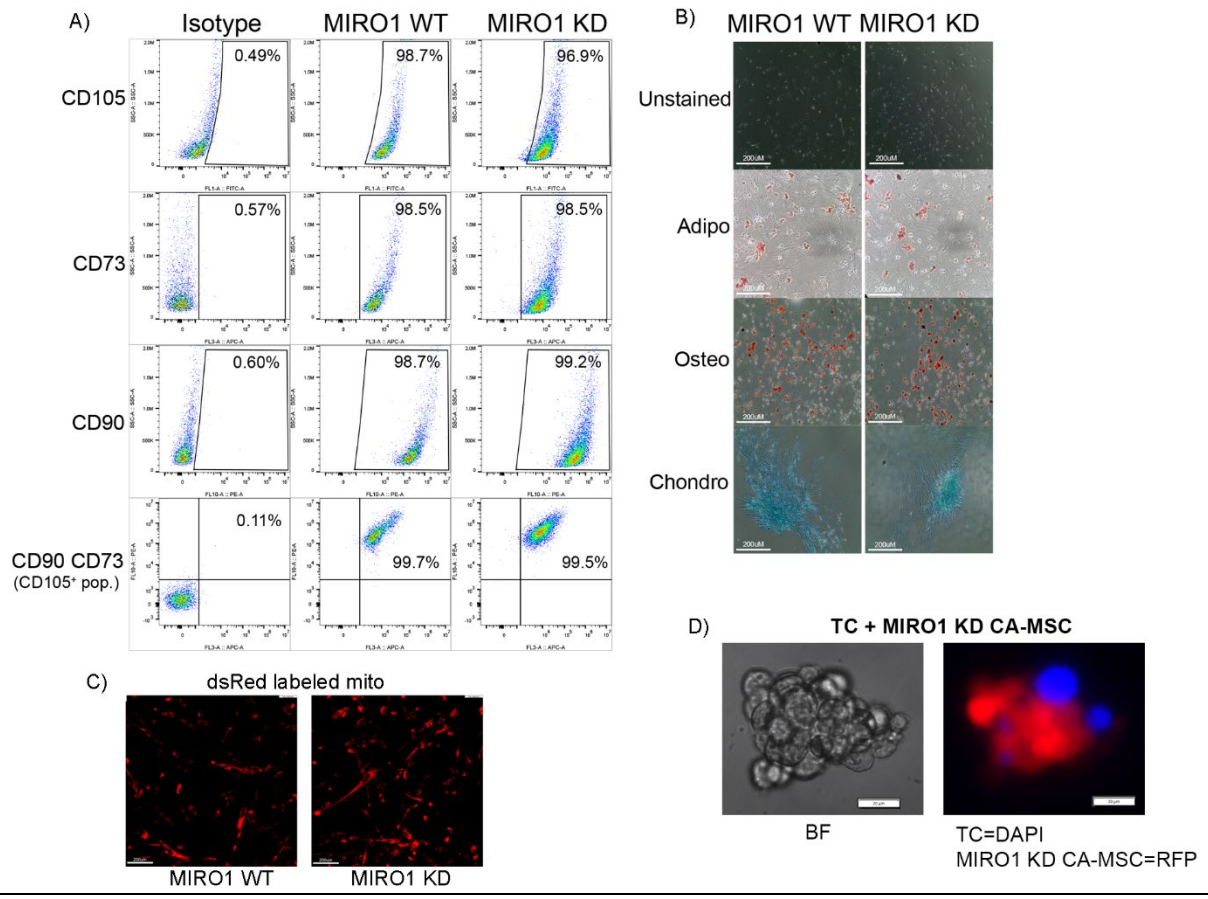

Figure S5. Validation of MSC surface marker expression and trilineage differentiation potential in wild type and MIRO1 knockdown CA-MSCs, related to Figure 6. Representative plots showing A) MSC surface marker expression in wildtype and MIRO1 knockdown CA-MSCs. B) Trilineage differentiation assay showing Oil Red O, Alizarin Red S and Alcian Blue staining in wildtype and MIRO1 knockdown CA-MSCs differentiated into adipocytes, osteocytes and chondrocytes, respectively. C) Deep red live mitochondria stain in MIRO1 WT vs MIRO1 KD CA-MSCs demonstrating similar pattern, amount and distribution of mitochondria. D) MIRO1 KD CA-MSCs labeled with RFP retain the ability to bind to tumor cells (stained with DAPI) and form heterocellular spheres under non-adherent conditions.

Number of Unique Barcodes and Reads from Tail-Vein Injection Model

Condition and Site	Number of Barcodes	Number of Reads	Number of Barcodes/ug DNA
TC + CA-MSC Lung	9410	392918657	22.61
TC + CA-MSC Abdomen	4623	326735198	18.23
TC + CA-MSC Liver	2161	262589084	2.95
TC Lung	1641	151035028	5.14
TC Liver	1238	143062065	2.33

Table S1, related to Figure 1: Shows the number of barcodes and number of total reads recorded across each site and condition in a tail vein injection model. These values correspond to the Sankey visualizations in Figure 1E-G**.**

Number of Reads in CA-MSC Alone vs MIRO1 Knockdown by Sample

Mouse, Condition, and Site	Number of Reads	Genomic DNA in Sample (μg)	Number of Reads (normalized by amount of μg Genomic DNA by sample)
M1 CA-MSC Primary	77886193	131.6	592065.3
M1 CA-MSC Liver	65703374	22.9	2874163.3
M2 CA-MSC Primary	73223004	71.4	1024958.1
M2 CA-MSC Liver	67607026	23.6	2870786.7
M3 MIRO1 Primary	75238821	42.6	1766169.5
M3 MIRO1 Liver	64306171	83.6	769120.6
M4 MIRO1 Primary	66617832	118.2	563745.7
M5 Tumor Only	1049474	66.6	15748.4

Table S2, related to Figure 7: Shows the number of reads for each site by sample in each mouse in *in vivo* MIRO1 knockdown and CA-MSC alone models. The number of reads were divided by the μg DNA in each sample to calculate a normalized number of reads such that different sites could be compared.

Video S1:
Real-time microscopy of CA-MSCs with GFP+ mitochondria and tumor cells demonstrating transfer of GFP+ CA-MSC mitochondria to adjacent tumor cells. Both cells types are stained with RFP-actin.